Solid State NMR and Wide Angle X-ray Diffraction Studies of Supercritical Fluid CO_2-Treated Poly(ethylene terephthalate)

Shi Bai, Jian Zhi Hu, Ronald J. Pugmire, and David M. Grant*

Department of Chemistry, University of Utah, Salt Lake City, Utah 84112

Craig M. V. Taylor,* James B. Rubin, and Eric J. Peterson

Los Alamos National Laboratory, Los Alamos, New Mexico 87545

Received October 14, 1997; Revised Manuscript Received July 7, 1998

ABSTRACT: Poly(ethylene terephthalate) (PET) was treated with supercritical fluid (SCF) carbon dioxide to study crystallization of this polymer under SCF conditions. Solid state NMR spectroscopy and wide angle X-ray diffraction (WAXD) detected dramatic changes in the PET molecular structure and motion after treatment. To fit WAXD data, the powder diffraction pattern for crystalline PET was calculated and is reported here for the first time. The WAXD results indicate an increase in crystallinity from essentially zero in the as-received sample to 62% in the SCF-treated sample. This large increase in the crystallinity of the SCF-treated PET was verified by the NMR relaxation measurements. The X-ray crystallite size, obtained from WAXD, was compared with those obtained from NMR proton spin diffusion measurements. The ^{13}C signals for aliphatic carbons (centered at 61.5 ppm) in the PET crystalline domain were resolved for the first time in a ^{13}C cross polarization/magic angle spinning spectrum (CP/MAS) due to the SCF treatment. The ^{13}C chemical shift tensors for PET were determined experimentally and were also compared to theoretical ab initio calculations. The anisotropic chemical shift data were then interpreted in terms of changes in the molecular conformation in PET as a result of SCF CO_2 treatment. It was found that the SCF CO_2 treatment is an effective method for enhancing the crystallinity of PET. These results in PET strongly support the previously proposed model for the existence of three motional regimes; crystalline, rigid amorphous, and mobile amorphous.

Introduction

Supercritical fluids (SCF's), as alternative solvents, have tremendous potential for the modification and processing of polymers,[1] as they offer many advantages over conventional organic solvents.[2−4] The solvent strength of SCF's can be tuned over a wide range by changing temperature and pressure. Thus, the degree of polymer swelling and partitioning of penetrants can be adjusted. The gaslike viscosity of SCF's results in higher possible flow rates. The near-zero surface tension makes supercritical fluids essentially infinitely wetting. The above factors, coupled with an extremely high diffusion rate, enhance the kinetic absorption of penetrants. Near its critical point (31 °C and 72 bar), CO_2 has a solubility in many polymers which is as high as that of typical organic liquid-swelling agents.[5] Finally, SCF solutions, especially CO_2, have clear environmental advantages over typical organic solvents.

The use of gaseous and liquid carbon dioxide to lower the glass transition temperature (T_g) of various polymers has been extensively studied.[6−9] It has also been demonstrated that SCF CO_2 has a strong plasticizing effect.[2−4,10,11] These studies have shown that the crystallization rates may be increased in CO_2 by higher temperatures and pressures. Poly(ethylene terephthalate) (PET) has been used as an example in several of these studies.[3,4,6]

Gas sorption in polymers, a purely physical phenomenon, is generally considered to play an important role in these crystallization processes. For instance, isothermal sorption of a gas into a polymer can result in a decrease in T_g which is proportional to the amount of gas sorbed. The T_g values for PET containing dissolved CO_2 at elevated pressures were estimated by Chiou et al.[6,7] using differential scanning calorimetry. The glass transition temperatures were found to be 35 °C at 35.5 bar and 52 °C at 20.2 bar. The CO_2-induced crystallization kinetics for amorphous PET were determined by Mizoguchi et al.[11] at 50.7 bar and the temperatures 35, 65, and 85 °C using IR spectroscopy and bulk polymer density measurements. The rate of crystallization was found to increase approximately 1 order of magnitude as the temperature was raised from 35 to 65 °C and again from 65 to 85 °C. The kinetics of CO_2 sorption in PET at pressures up to 50.7 bar and temperatures up to 65 °C were determined by Kamiya et al.[12] using a gravimetric technique. Kamiya reported a CO_2-induced crystallinity of approximately 29 vol %, in agreement with subsequent experiments under similar conditions.[13] Evidence[14,15] of an electron donor−acceptor complex between CO_2 and electron-donating polymers has been observed by IR. PET follows this model because the carbonyl oxygen acts as an electron donor. The CO_2-induced crystallization of PET has been reviewed by Hirose et al.[16] and Lambert and Paulaitis.[13]

Differential scanning calorimetry (DSC), density measurement, and wide angle X-ray diffraction (WAXD) are often used to characterize polymer samples before and after CO_2 treatments. Solid state NMR is a premier tool for exploring the detailed structural and dynamic information of polymers,[17,18] but it has not previously been used to characterize polymers following SCF treatment. Earlier solid-state NMR studies on PET focused on molecular motions and their effect on spin relaxation measurements.[19,20] Recently Chmelka et al.[21] reported that molecular chain orientational order

* Corresponding authors.

10.1021/ma9715031 CCC: $15.00
Published on Web 12/05/1998

in mechanically altered PET samples (fibers and films) can be extracted by multidimensional DECORDER NMR experiments. Orientational information in PET fibers has also been studied with static spectra obtained at different angles between the magnetic field direction and the draw direction of a uniaxially oriented ^{13}C-labeled PET sample.[22] NMR relaxation measurements and line shape analysis by Veeman and co-workers[23] utilize a model with three distinct regions, NMR crystalline, rigid NMR amorphous, and mobile NMR amorphous. This three-region model for PET was based on earlier work by Havens and VanderHart.[24]

In this work, a variety of solid state NMR techniques and WAXD were used to study the treatment of PET powder samples with SCF CO_2. The crystalline volume fraction and average crystallite sizes of the PET samples before and after CO_2 treatments were obtained by WAXD. The molecular motions for both as-received and SCF-treated PET samples were investigated by changes in the ^{13}C T_1, ^{13}C $T_{1\rho}$, and ^1H $T_{1\rho}$ parameters. The NMR crystallinity of the PET polymer was obtained from the measurements of ^{13}C $T_{1\rho}$ using a three-dimensional diffusion model. The principal values of the ^{13}C chemical shift tensors for the SCF CO_2-treated PET sample were measured by a two-dimensional magic angle turning (2D MAT) experiment.[25−27] Noticeable differences in the principal values were observed for the two aliphatic carbon peaks of this SCF-treated PET. Anomalies in the principal values of PET aliphatic carbons reported in the literature may be understood in terms of these new results. Compared with those from ab initio calculations, the principal values for aliphatic carbons suggest that the trans conformation dominates the crystalline domain. Conversely, the gauche conformation dominates the amorphous domain.

Experimental Section

Samples. PET, lot no. 02019JF, was supplied by Aldrich Chemical Co. in the form of 5 mm pellets. The pellets were frozen in liquid nitrogen for 5 min prior to being ground to powders using a Regal electric coffee grinder. Sieving (50−100 mesh) was carried out using Fisher Scientific "MESH" series sieves. Samples to be treated with the SCF CO_2 were loaded into a 5 L CF Technologies (Hyde Park, MA) extractor. The temperature and pressure of the SCF treatment were 70 °C and 208 bar, respectively. The sample was held at this temperature and pressure for 90 min. Then the pressure was reduced isothermally at a constant rate to atmospheric pressure over a period of 60 min. The thermally treated PET sample was prepared by heating the sample at 70 °C for 150 min at atmospheric pressure. After treatment, samples were unloaded from the extractor and left at ambient conditions for at least 7 days before NMR measurements. For convenience, the as-received, thermally treated, and SCF-CO_2-treated PET samples are designated as PET0, PET1, and PET2, respectively.

The PET1 sample was prepared to separate purely thermal effects from those attributable to the SCF treatment at the same temperature. An entirely thermal effect on crystallization should be very small, if it exists at all. PET is a slowly crystallizing polymer,[28] and an extrapolation of experimental data[13,28] indicates that the crystallization half time $t_{1/2}$ for PET at 70 °C is expected to be 63 h. This half time is at least 25 times longer than the thermal treatment time (150 min) in this study.

WAXD Measurements. The PET samples were analyzed using a Scintag XDS2000 X-ray diffractometer equipped with a graphite monochromator and a horizontal sample carousel having six rotating sample cups. The individual cups are 2.6 cm in diameter and 0.3 cm in depth. PET powder was pressed into the cup and the top surface planed with a glass slide. Diffraction data were collected in the range $10 < 2\theta < 80°$ with the step size 0.03° (2θ) and the counting time 25 s per step using Cu Kα radiation. The diffraction patterns were deconvoluted using profile fitting software[29] which uses a Pearson VII function to fit individual peaks.

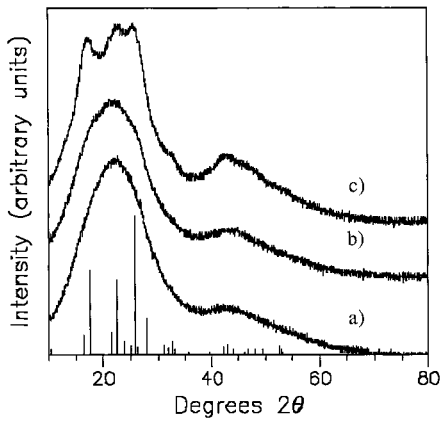

Figure 1. WAXD patterns of PET samples: (a) as-received sample; (b) thermally treated PET sample; (c) SCF CO_2-treated PET sample. Along the abscissa are the calculated peak positions and relative intensities for 100% crystalline PET.

NMR Spectroscopy. ^{13}C CP/MAS measurements were performed on a Chemagnetics CMX-100 spectrometer using a 7.5 mm PENCIL rotor probe operating at a ^{13}C frequency of 25.152 MHz. Standard pulse sequences for the ^{13}C CP/MAS, inversion recovery, and $T_{1\rho}$ experiments for both ^1H and ^{13}C were used, using a sample spinning speed of 4.1 kHz. The ^{13}C CP/MAS and spin−lattice relaxation experiments employed a proton 90° pulse length of 4.0 μs, a recycle time of 2 s, and a crosspolarization time of 2 ms.

The 2D MAT experiments were performed on a VXR200 spectrometer operating at the ^{13}C frequency 50.309 MHz using the triple-echo[26] sequences on a 12 mm home-built probe with the sample rotor spinning rate 16.8 ± 0.1 Hz. The rf pulses were synchronized to $^1/_3$ of the rotor cycle with our rotor synchronization device.[27] A proton 90° pulse length of 5.0 μs and a contact time of 2 ms were used. The spectral widths in acquisition and evolution dimensions were 60 and 6.67 kHz, respectively. A FID of 256 complex points was acquired. There were 60 complex increments in the evolution dimension, resulting in a resolution of about 100 Hz in this dimension, and 512 scans with the recycle delay time 4 s yielded spectra with good signal-to-noise ratios. The 2D data sets were processed on a VAX station 3100 computer. The powder spectrum for each chemically distinctive nucleus was obtained by taking a sliced spectrum at the center of the isotropic chemical shift position. Individual powder patterns were fit using the POWDER software.[30]

Results and Discussion

A. Crystalline Volume Fraction and Crystallite Size from WAXD. The WAXD patterns for the three PET samples (PET0, PET1, and PET2) were analyzed for both crystalline volume fraction and average crystallite size. The results are shown in Figure 1. For PET0, two broad peaks were observed, corresponding to the first- and second-order amorphous halos. For PET2, somewhat narrower peaks were superimposed onto the amorphous halos. To fit the diffraction patterns, starting values of peak position and intensity for crystalline PET are required. The powder diffraction pattern for an isotropic, 100% crystalline PET was calculated using the structure refinement data of Fu et al.[31] and the POWD12 program of Smith.[32] The resulting peak positions and intensities are shown along the abscissa in Figure 1. The peak positions and relative

Table 1. Calculated Powder Diffraction Pattern for PET, Based on the Structure Data of Fu et al.[31]

2θ	relative intensity	(h,k,l)
10.26	3	(0,0,1)
16.24	13	(0,−1,1)
17.60	61	(0,1,0)
21.37	16	(−1,1,1)
22.54	54	(−1,1,0)
23.89	9	(0,1,1)
24.92	6	(−1,1,2)
25.80	100	(1,0,0)
26.36	5	(−1,0,3)
27.88	26	(1,−1,1)
31.12	7	(0,0,3)
32.02	4	(−1,−1.3)
32.59	9	(0,−2,1)
33.07	3	(−1,2,1)
33.09	3	(1,0,1)
35.68	2	(1,−1,2)
39.55	2	(−2,1,2)
42.27	5	(0,−2,4)
42.84	7	(−1,0,5)
43.98	3	(−2,1,4)
46.00	2	(−2,1,0)
46.65	3	(−1,−2,4)
48.16	3	(−2,0,5)
49.37	3	(−1,3,1)
49.50	2	(−1,−2,1)
52.49	2	(−2,3,1)
52.52	6	(2,−1,1)
53.03	3	(2,0,0)
53.12	2	(0,0,5)

Table 2. Degree of Crystallinity (X_C) and Crystalline Size of the PET Polymer from the WAXD Measurements

sample	avg crystalline volume fraction (%)	avg crystalline size[b] (Å)
PET0	0	10 (5)
PET1	<5	c
PET2	62 (10)[a]	42 (5)[a]

[a] The data in parentheses are the standard errors. [b] Data were obtained using the Scherrer equation. [c] Measurement was not carried out.

intensities for the calculated pattern are given in Table 1. These parameters were used to fit the experimental diffraction patterns in the range $10 < 2\theta < 36.5°$. The resulting integrated peak intensities were used to estimate the polymer crystallinity. Only the six most intense crystalline peaks were used in a method similar to that of Huisman and Heuvel[33] in their analysis of PET yarns. The volume percent crystallinity was found by dividing the sum of the six integrated crystalline peaks by the integrated sum of the six crystalline peaks plus the single amorphous peak. The volume percent crystallinities for PET0, PET1, and PET2 are listed in Table 2.

The data in Table 2 indicate that both the as-received (PET0) and thermally treated (PET1) polymer samples are essentially amorphous. A slight increase in crystallinity is found for PET1 upon the thermal treatment, indicating that the thermal effect at 70 °C is indeed small for PET. However, the SCF CO_2-treated PET sample (PET2) has a crystallinity of 62 ± 10%. It is reported[6,7] that the crystallinity increases 24−29% for PET by sorption of CO_2 gas at pressures between 20.3 and 35.5 bar. The dramatic increase (62%) in crystallinity for PET by SCF CO_2 treatment for only 90 min shows the advantages of SCF CO_2 treatment over the treatment using gas-phase CO_2.

Also shown in Table 2 are the X-ray crystallite sizes for the PET0 and PET2 samples, estimated from the peak deconvolution and using the Scherrer equation. It is noted that the crystalline size is increased from 10 Å for PET0 to 42 Å for PET2 due to the SCF CO_2 treatments.

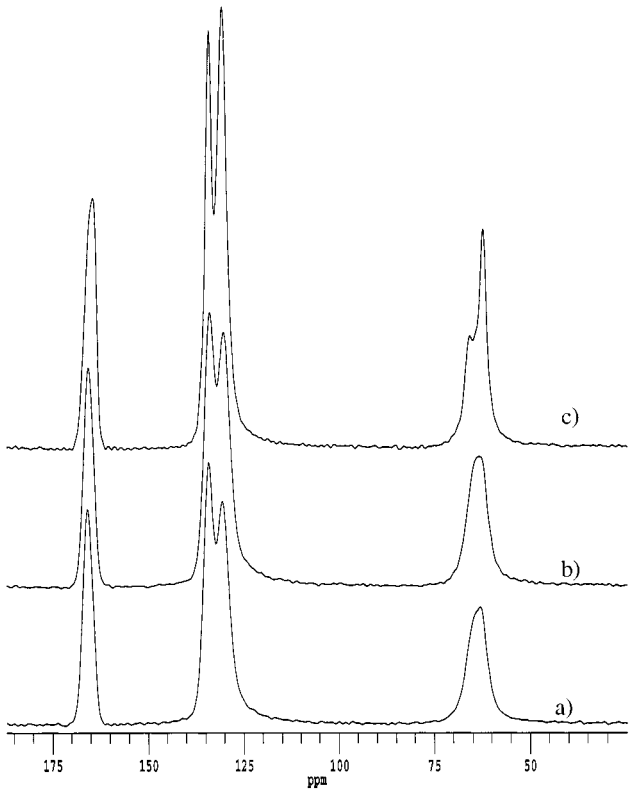

Figure 2. CP/MAS spectra of PET samples: (a) as-received sample; (b) thermally treated PET sample; (c) SCF CO_2-treated PET sample. All chemical shift values are referenced to TMS. Generally narrowed lines are observed for the SCF CO_2-treated PET sample, and a new peak with the chemical shift 61.5 ppm is noted in the aliphatic carbon region. The downfield peak in part c for aliphatic carbons is at 65.3 ppm. The sharp peak and the left shoulder for aliphatic carbons in part a are at 62.5 and 65.3 ppm, respectively.

^{13}C CP/MAS Spectra. The ^{13}C CP/MAS spectra of three PET samples, as-received (PET0), thermally treated (PET1), and SCF CO_2 treated (PET2), are given in Figure 2 as a, b, and c, respectively. Notice the effect of sample treatment on the spectral resolution. The narrower lines in the spectrum of PET2 compared with those in the spectrum of PET0 are attributed to an increase in the crystallinity. The intensity of the amorphous phase carbon peaks also decreases in PET2 compared to PET0, resulting in a distinctive component of higher resolution centered at 61.5 ppm. Similar line widths are noted in Figure 2 for both the PET0 and the thermally treated PET1. The broader lines observed for PET0 and PET1 suggest a larger distribution of isotropic chemical shifts partially due to greater heterogeneity and a larger orientational distribution of polymer molecules. Two distinguishable resonances for aliphatic carbons were observed in the PET2 spectrum at 61.5 and 65.3 ppm, indicating the structural modification resulting from SCF CO_2 treatment. The splitting observed in PET2 appears to be independent of minor changes in both the strength and offset of the decoupler field. These observations suggest the aliphatic carbons in treated PET occupy at least two major magnetically nonequivalent positions. The line shape in Figure 2a for the aliphatic carbons in PET0 also appears to consist

Table 3. Experimental[a] and *Theoretical* Principal Values of the Carbon Chemical Shift Tensors of PET

sample	δ_{11}	δ_{22}	δ_{33}	δ_{iso} avg	MAS	ref
			aliphatic			
PET0	87	74	33	65	62.5	this work
PET2	86	75	33	65	65.3	this work
	87	74	25	62	61.5	this work
PET[b]	87	76	22	62		21
	85	77	29	64		34
	87	75	20	61		35
	80	80	28	63		36
D95(trans)[c]	108	75	16	66		
D95(gauche)	107	75	35	72		
			Protonated Aromatic			
PET0	221	154	14	130	130.4	this work
PET2	221	155	14	130	130.3	this work
PET[b]	223	158	13	131		21
	220	164	10	131		34
	223	159	11	131		35
	226	153	15	131		36
D95(trans)	219	147	8	125		
D95(gauche)	219	146	8	124		
			Nonprotonated Aromatic			
PET0	232	145	25	134	133.8	this work
PET2	235	146	27	136	133.5	this work
PET[b]	228	146	31	135		21
	226	144	32	134		34
	230	145	26	134		35
	226	153	15	131		36
D95(trans)	204	134	26	122		
D95(gauche)	205	136	25	122		
			Carbonyl			
PET0	255	124	110	163	165.2	this work
PET2	257	124	110	163	165.0	this work
PET[b]	252	126	113	164		21
	250	127	117	165	34	
	252	131	107	163	35	
	250	122	122	165		36
D95(trans)	274	129	123	175		
D95(gauche)	276	126	124	175		

[a] All experimental chemical shift principal values are in ppm referenced from TMS. [b] PET samples are described in the related references. [c] All theoretical chemical shift principal values are in ppm and converted from screening values. TMS was used as a reference in these calculations.

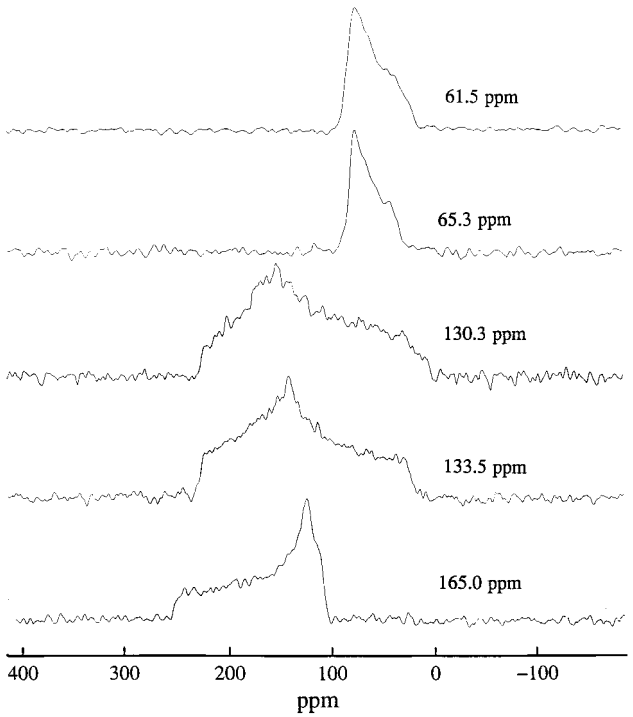

Figure 3. Anisotropic projections of the 2D MAT experiment for the SCF CO_2-treated PET. The numbers in the spectra correspond to the isotropic shifts. The spectra from the top to the bottom are the aliphatic (trans), aliphatic (gauche), protonated aromatic, nonprotonated aromatic, and carbonyl carbons.

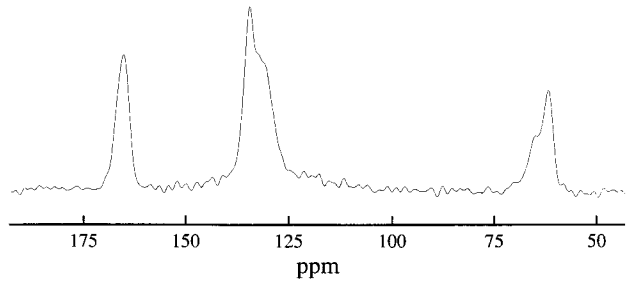

Figure 4. Isotropic projection of the 2D MAT experiment for the SCF CO_2-treated PET. The CP/MAS resolution of aliphatic carbons is preserved in the MAT experiments.

of a peak at 62.5 ppm with a left shoulder at 65.3 ppm. According to the WAXD results, PET0 is essentially amorphous while PET2 is highly crystalline. Upon comparison with the spectrum of PET0, a new peak at 61.5 ppm for PET2 appears to be a crystalline peak. By deconvoluting the aliphatic carbon peak, Veeman et al.[23] noted a broad, low-field amorphous component shifted 1.0 ppm downfield with respect to a narrow crystalline component. The peak with the chemical shift 62.5 ppm in the PET0 spectrum (Figure 2a) is likely to be the component observed by Veeman et al, because it is about 1.0 ppm shifted downfield with respect to the 61.5 ppm peak for PET2. The peaks at 65.3 and 62.5 ppm are thus assigned to the rigid amorphous and mobile amorphous domains, respectively. More evidence from relaxation and chemical shift anisotropic measurements, to be addressed later, supports this argument.

Chemical Shift Principal Values. To further explore the differences between the two peaks observed for PET2, 2D MAT experiments have been performed for PET0 and PET2 from which the chemical shift anisotropic information of each individual carbon may be extracted. Table 3 reports experimentally determined principal values for the PET chemical shift tensors as well as the theoretical results, given in *italic* font. Previously reported values in the literature are included for comparison. The powder patterns of the individual carbons in PET2, from which the principal values were obtained, are given in Figure 3. These powder pattern slices were obtained from MAT data at the isotropic chemical shifts indicated. The overall isotropic projection from the MAT experiment is presented for PET2 in Figure 4 to demonstrate that the CP/MAS resolution of the aliphatic carbon in PET2 is retained in the 2D MAT experiment.

The chemical shift tensors, along with the WAXD data, allow us to assign the two aliphatic carbon peaks observed in PET2. The two aliphatic carbon tensors differ by about 8 ppm in the δ_{33} component (see Table 3). The chemical shift principal values of the 65.3 ppm peak (δ_{11}, δ_{22}, and δ_{33} at 86, 75, and 33 ppm, respectively) agree with those of the PET0 tensor (87, 74, and 33 ppm) within experimental error. These are assigned to the *rigid* amorphous aliphatic carbons in PET for the reasons discussed later in this paper. The similarity between chemical shift tensors for aliphatic carbons in

Table 4. Single and Double Exponential $T_1(^{13}C)$ Relaxation Results in the Laboratory Frame

sample	T_{1A} (s)	M_A (%)	T_{1B} (s)	M_B (%)
		Aliphatic		
PET0	15.2 (3.5)[a]	42.7 (4.0)	1.0 (0.1)	57.3 (3.2)
PET2 (61.5 ppm)	14.2 (1.3)	68.8 (5.5)	0.5 (0.1)	31.1 (3.1)
PET2 (65.3 ppm)	16.0 (2.4)	65.1 (5.7)	0.6 (0.2)	34.9 (4.6)
		Protonated Aromatic		
PET0	20.9 (2.1)	86.4 (4.6)	1.5 (0.9)	13.6 (1.5)
PET2	27.3 (2.1)	87.1 (4.2)	1.0 (0.4)	12.8 (1.8)
		Nonprotonated Aromatic		
PET0	21.7 (1.4)	90.3 (3.6)		
PET2	29.3 (2.4)	90.2 (6.7)		
		Carbonyl		
PET0	26.5 (1.4)	93.4 (3.2)		
PET2	38.2 (3.6)	101.9 (1.5)		

[a] Data in parentheses are the standard errors in relaxation parameters.

PET0 and those in PET2 with an isotropic shift of 65.3 ppm appears to suggest the as-received PET0 shares a similar molecular structure to that for the downfield line in PET2. It is very difficult to extract chemical shift tensor information for mobile amorphous carbons because of the wide distribution of isotropic chemical shifts. The other tensor, with the principal values $\delta_{11} = 87$, $\delta_{22} = 74$, and $\delta_{33} = 25$ ppm, is assigned to the crystalline aliphatic carbons. These assignments are consistent with the CP/MAS results given in the preceding section.

Previous measurements[21,34−36] of the principal values of the ^{13}C chemical shift tensors in PET are tabulated in Table 3. In general, our measurements agree with the literature values for all carbons. The δ_{11} and δ_{22} values for aliphatic carbons are within experimental error of the literature values. The δ_{33} literature values, however, range from 20 to 29 ppm[21,34−36] (see Table 3). In this work, the δ_{11} and δ_{22} values for the aliphatic carbons remained unchanged in both crystalline and amorphous PET, but the δ_{33} value is reduced from 33 ppm in the amorphous to PET 25 ppm in the crystalline PET. Thus the range of δ_{33} values in the literature may be attributed to morphological differences in the samples.

The reduced span of the aliphatic tensor in PET2 between crystalline and amorphous is likely caused by both the molecular conformation changes and enhanced molecular motion. Narrowing induced by increased molecular motion, however, usually does not involve changes in the isotropic chemical shift.[37] Hence, it is a conformational change that offers the preferable explanation for most of the differences. Theoretical calculations were performed in order to explore the possible origin of the significant differences existing between the chemical shift tensors of crystalline and rigid amorphous aliphatic carbons. DFT calculations, performed with Gaussian[38] 94 and GIAO[39](gauge invariant atomic orbitals) methods, employ the standard Dunning[40] D95 basis set. The calculations use geometry parameters determined by X-ray diffraction.[41] Carbon chemical shift principal values have been calculated for both the trans and gauche OCCO dihedral angular conformations, and the results are listed in Table 3. Both experimental and theoretical chemical shift principal values of protonated, nonprotonated, and carbonyl carbons do not change with changing conformation, as might be expected. The δ_{11} and δ_{22} values for the aliphatic carbons also do not vary significantly for the various conformations. However, δ_{33} changes from 35 ppm for the gauche conformation to 16 ppm for the trans conformation in the theoretical calculations, and this trend is similar to that observed experimentally. This change in δ_{33} suggests that the trans and gauche conformations are enhanced, respectively, in the crystalline and amorphous aliphatic tensors.

The chemical shift tensor orientations for aliphatic carbons have been previously determined using the separated local field method in both PET fiber and film.[21] The orientation of chemical shift tensors for aromatic carbons is consistent with that of other organic compounds where δ_{33} is aligned along the axis normal to the rings and δ_{11} is aligned along the C−H or C−C bond direction radial to the ring.

***$T_1(^{13}C)$* Measurements.** The standard inversion recovery pulse sequence was used to measure spin−lattice relaxation times in the laboratory frame for the samples PET0 and PET2. The delay times ranged from 0.01 to 300 s. The results are tabulated in Table 4. The T_1 values of the two distinguishable aliphatic carbon lines in PET2 are listed separately in the table as 61.5 ppm and 65.3 ppm, corresponding to the upfield and downfield resonances, respectively. Double-exponential terms are needed to fit the partially relaxed magnetization data both for aliphatic and for aromatic protonated carbons. However, a single-exponential term was adequate for fitting the magnetization data of nonprotonated aromatic and carbonyl carbons. For aliphatic carbons, no significant changes in T_1 were observed between PET0 and PET2. However the percentage of the longer relaxation component (14−16 s) increases from 42.7 for PET0 to 65.1 and 68.8 for the two aliphatic peaks of PET2. The PET2 aliphatic carbon resonance at 65.3 ppm shares similar relaxation times with the resonance at 61.5 ppm. Thus if the signal at 65.3 ppm is indeed from the amorphous domain, as discussed above, it must arise from the *rigid* amorphous domain because of this similar ^{13}C T_1 relaxation behavior. The shorter relaxation time components are most likely from the *mobile* amorphous domain. Figure 5 shows several partially relaxed spectra for the aliphatic carbons in PET2 demonstrating differential relaxation rates between the mobile amorphous (center peak) and rigid amorphous (left shoulder) domains. The resolution of the outer two spectral peaks becomes much better at delay times from 6 to 10 s, where the signal resulting from the fast (amorphous) relaxation component is too small or inverted from the outer two resonances. At the delay time 50 s, the signal of the fast relaxation component (central line) has definitely recovered, while the outer shoulders (65.3 and 61.5 ppm) are still

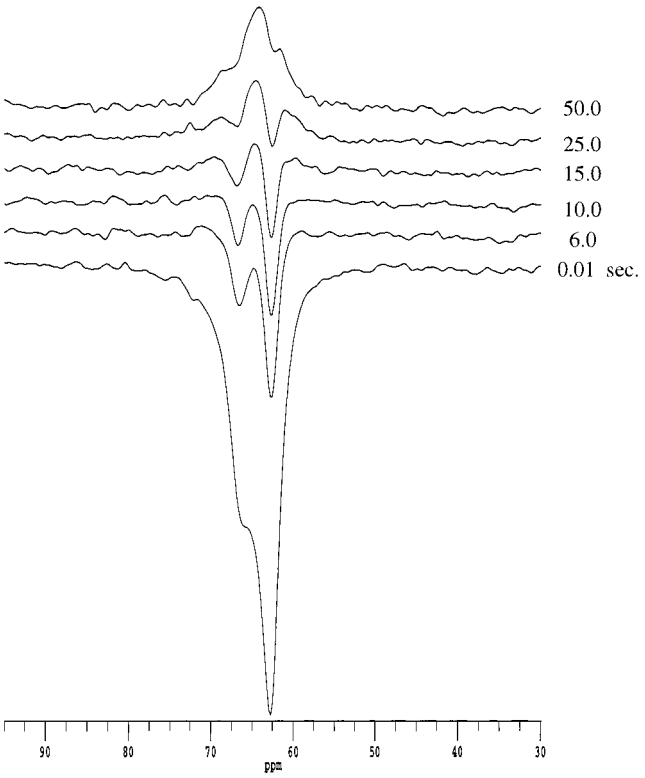

Figure 5. Partially relaxed aliphatic carbon spectra of the SCF CO_2-treated PET in an inversion recovery experiment. Higher resolution is observed for spectra with the delay times 6−10 s. The broader line in the spectrum with the delay time 50 s is the signal from mobile amorphous phases.

recovering. The rapidly relaxing nature of the broad line at 62.5 ppm indicates that some aliphatic carbons are located in the mobile domain and thus have fast relaxation rates. This explanation is consistent with a three-region motional model. It is well-known that only fast molecular motions with correlation times less than 10^{-8} s contribute to the spin−lattice relaxation rate in the laboratory frame for the ^{13}C nucleus. The results of T_1 relaxation measurements show that the crystalline and rigid amorphous aliphatic carbons have similar motional behaviors, while the mobile amorphous carbons behave somewhat differently. It is interesting to note that the MAS chemical shift for the aliphatic carbons in PET0 is centered at 62.5 ppm (see Table 3), which is the same as the shift for the fast relaxing component in PET2. This similarity in chemical shift indicates that the mobile amorphous phase dominates the structures in PET0. Since PET0 has δ_{33} values similar to those calculated for the gauche conformation (cf. Table 3), it is assumed that the mobile amorphous domain is dominated by the gauche conformation in the aliphatic carbons.

The similar relaxation parameters (cf. Table 4) observed for the aromatic carbons between PET0 and PET2 indicate that SCF CO_2 treatments do not significantly affect the molecular motions of the aromatic carbons on the NMR time scale.

***$T_{1\rho}$*(^{13}C) Measurements.** Spin−lattice relaxation in the rotating frame, $T_{1\rho}(^{13}C)$, may be studied with molecular motional parameters in polymers observed at a relatively high field strength.[20,23] The results of $T_{1\rho}$-(^{13}C) measurements for all carbons in PET0, PET1, and PET2 are listed in Table 5. All measurements correspond to the field strength ν_1 = 62.5 kHz. It was found that double-exponential terms again were needed to fit the relaxation data for aliphatic, protonated aromatic, and nonprotonated aromatic carbons, while only a single-exponential term was required to fit the magnetization data for carbonyl carbons. The complexity in the relaxation processes for nonprotonated carbonyl and aromatic carbons as recognized by Veeman et al.,[23] has focused our attention on the relaxation behavior of aliphatic carbons and protonated aromatic carbons.

Figure 6 shows the decay of the aliphatic carbon magnetization as a function of delay time τ for PET0, PET1, and PET2 at the field strength ν_1 = of 62.5 kHz. PET0 and PET1 have similar decay patterns, while a significantly different response is observed for PET2. Figure 6 indicates that thermal treatment under the conditions studied introduced only small changes, while the SCF CO_2 treatment introduced dramatic changes in the molecular motions of PET. The two relaxation times found for aliphatic carbons in PET0 were 2.2 and 22.7 ms, with fractions of 36.5 and 63.5%, respectively. Similarly, the relaxation times observed for PET1 were 2.1 and 26.1 ms, with fractions of 37.9 and 62.1%, respectively. These relaxation parameters agree very well with those previously obtained by Veeman et al. for amorphous PET yarns at ν_1 = 78 kHz, suggesting that the as-received and thermally treated PET samples are amorphous polymers. The WAXD results (Table 2) confirm that the untreated and thermally treated PET samples (PET0 and PET1) are indeed amorphous polymers. The double-exponential behavior of ^{13}C $T_{1\rho}$ suggest that there exist two motionally different domains in the untreated amorphous PET sample: the *rigid* and *mobile* amorphous domains corresponding to the longer and shorter relaxation times, respectively.

Table 5 shows the results of fitting the magnetization data for PET2 with double-exponential terms. The relaxation time constants 55.8 ms (62.8%) and 3.9 ms (37.2%) were observed for the aliphatic carbons. If the three-domain structural model is used, the relaxation time 3.9 ms is just the average value of the relaxation times for aliphatic carbons in the NMR rigid and mobile amorphous domains. The component with 55.8 ms is, therefore, from the NMR crystalline domain, as this component is induced by the SCF CO_2 treatments. As the three motional regimes (crystalline, rigid amorphous, and mobile amorphous) exist for the semicrystalline PET polymers, magnetization data fitting with three exponential terms was employed for PET2. The results are listed in Table 5. The relaxation times 22.0 and 2.5 ms from the amorphous domains, respectively, agree well with those of 22.7 and 2.2 ms observed for PET0. The relaxation time 54.6 ms (from the crystalline domain, cf. Table 5) is similar to that of 55.8 ms from the double-exponential term fit for PET2. The NMR crystallinity of aliphatic carbons M_C, which is the fraction of the 54.6 ms component, is found to be 51.4% and qualitatively agrees with that measured by the WAXD method (62 ± 10%; cf. Table 2). The fractions of rigid (21.6%) and mobile (26.9%) amorphous aliphatic carbons are basically evenly distributed. The three-exponential fit for PET2 and the double-exponential fit for PET0 are given in Figure 7, where the initial magnetization of the PET0 aliphatic carbons is normalized to 50 for better visual clarity. The dashed and solid lines in Figure 7 are the least-squares fits to the relaxation time data using two and three exponential

Table 5. Single-, Double-, and Triple-Exponential $T_{1\rho}(^{13}C)$ Relaxation Results

sample	$T_{1\rho A}(^{13}C)$ (ms)	M_A (%)	$T_{1\rho B}(^{13}C)$ (ms)	M_B (%)	$T_{1\rho C}(^{13}C)$ (ms)	M_C (%)
			Aliphatic			
PET0	22.7 (2.7)[a]	63.5 (4.8)	2.2 (0.6)	36.5 (4.7)		
PET1	26.1 (2.8)	62.1 (4.7)	2.1 (0.5)	37.9 (4.5)		
PET2[b]	55.8 (7.9)	62.8 (3.0)	3.9 (0.6)	37.2 (3.6)		
PET2[c]	22.0 (2.1)	21.6 (4.6)	2.5 (0.5)	26.9 (3.3)	54.6 (3.9)	51.4 (2.6)
			Protonated Aromatic			
PET0	45.6 (3.4)	67.5 (4.8)	2.5 (0.4)	32.5 (4.5)		
PET1	71.0 (8.1)	68.9 (2.4)	1.9 (0.4)	31.1 (2.5)		
PET2[b]	120.3 (10.5)	81.1 (1.6)	3.5 (0.6)	18.9 (1.5)		
PET2[c]	44.2 (2.8)	8.9 (3.2)	2.6 (0.4)	16.1 (0.9)	115.8 (4.1)	75.0 (2.6)
			Nonprotonated Aromatic			
PET0	98.2 (4.9)	86.4 (1.0)	1.7 (0.3)	13.6 (1.0)		
PET1	119.2 (11.3)	87.5 (1.4)	0.9 (1.3)	12.5 (1.5)		
PET2	155.7 (3.2)	94.7 (0.2)	1.1 (0.2)	5.3 (2.8)		
			Carbonyl			
PET0	123.1 (6.8)	94.8 (1.6)				
PET1	121.4 (6.0)	95.5 (0.5)				
PET2	120.5 (6.4)	100.9 (1.1)				

[a] Data in parentheses are standard deviations. [b] Double exponential decay fit. c) Fit with three exponential terms.

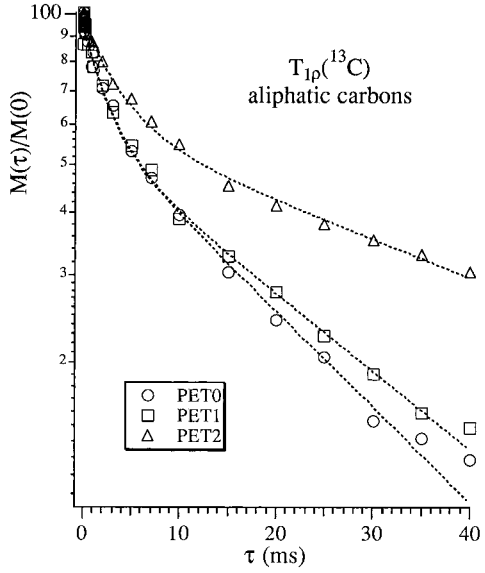

Figure 6. Aliphatic carbon magnetization decay patterns for the as-received, thermally treated, and SCF CO_2-treated PET samples in a $T_{1\rho}(^{13}C)$ experiment. The as-received and thermally treated samples have similar decay patterns. Aliphatic carbons in the SCF CO_2-treated PET decay much more slowly.

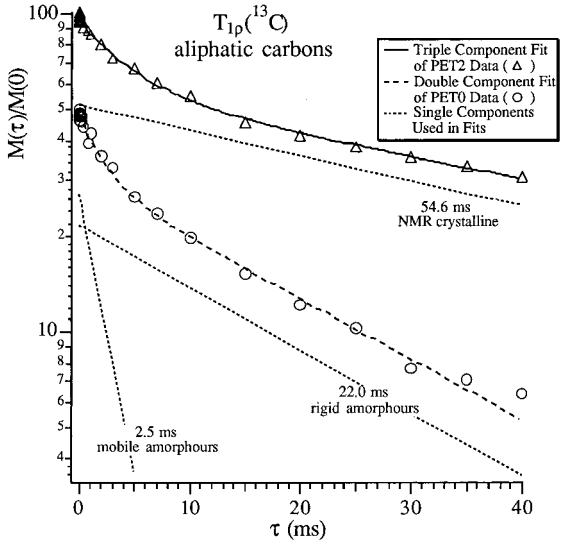

Figure 7. Aliphatic carbon magnetization decay patterns for the as-received and SCF CO_2-treated PET samples in a $T_{1\rho}(^{13}C)$ experiment. Double-exponential terms are needed to fit the magnetization data for the as-received PET0 (open circles), while three exponential terms are used to fit the magnetization data for the SCF CO_2-treated PET2 (open triangle). These respective fits are represented by the solid and dashed lines. The three dotted lines with the relaxation times 2.5, 22.0, and 54.6 ms are the decay components of the mobile amorphous, rigid amorphous, and NMR crystalline regions, respectively, and combine to give the composite fits. The 54.6 ms component appears only in the higher crystalline PET2 sample.

terms for PET0 and PET2, respectively. The dotted lines in the figure represent the three different relaxation components, corresponding to the NMR rigid amorphous, mobile amorphous, and crystalline domains.

The same data analysis for the aliphatic carbons was also applied to the protonated aromatic carbons in PET0 and PET2. The results are also listed in Table 5. An NMR crystallinity (M_C) of 75% was found for the protonated carbons of PET2, which once again agrees qualitatively with the WAXD results (cf. Table 2). The fraction of the mobile amorphous domain (16%) in PET2 is almost double that of the rigid amorphous domain (9%). The explanation of these observations is not entirely clear. For the nonprotonated carbons, the relaxation time of the long relaxation component increased from 98.2 ms for PET0 to 155.7 ms for PET2, and the fraction increased from 86.4% to 94.7%. However, the SCF CO_2 treatment has little effect on the ^{13}C relaxation parameter in the rotating frame for carbonyl carbons in PET.

***$T_{1\rho}(^1H)$* Measurements.** The proton relaxation times in the rotating frame for the PET samples were measured, and the magnetization decay patterns for PET0, PET1, and PET2 are given in Figure 8. The experimental magnetization data in the figure are the average of different carbons in PET, since the intrinsic $T_{1\rho}(^1H)$ relaxation times of chemically different protons are averaged by the effective spin−diffusion interactions.[23,24] The as-received and thermally treated PET samples share similar decay behavior where the signal intensity as a function of τ may be fitted using a single-exponential term. These observations are in agreement with the results of Veeman et al. for the amorphous PET. For the SCF CO_2-treated PET2, it is found that a double-exponential function was needed to fit the

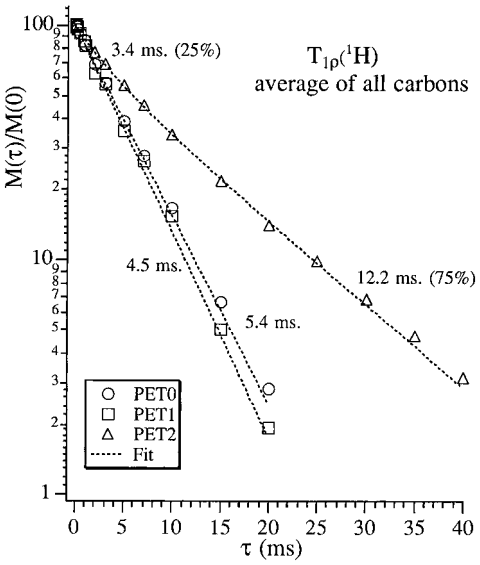

Figure 8. Average carbon magnetization decay patterns for the as-received, thermally treated, and SCF CO_2-treated PET samples in a $T_{1\rho}(^1H)$ experiment. A single-exponential term is used for the magnetization of both as-received and thermally treated PET samples. Double-exponential terms are needed to fit the magnetization of SCF CO_2-treated PET2. The dotted lines represent these fits.

Table 6. Single and Double-Exponential $T_{1\rho}(^1H)$ Relaxation Results

sample	$T_{1\rho A}(^1H)$ (ms)	M_A (%)	$T_{1\rho B}(^1H)$ (ms)	M_B (%)
PET0			5.4 (0.1)[a]	99.8 (0.2)
PET1			4.9 (0.1)	100.5 (0.5)
PET2	12.2 (0.4)	75.0 (3.5)	3.4 (0.4)	25.0 (2.5)

[a] Data in parentheses are standard deviations.

experimental data for the semicrystalline sample, which agreed well with previous observations.[23,42] The relaxation parameters from fitting the experimental data are tabulated in Table 6. It is clear from the table that the SCF CO_2 treatment introduced a new relaxation component with the relaxation time 12.2 ms and a mole fraction of 75%. The shorter relaxation time (3.4 ms) reflects the initial fast relaxation decay of magnetization in the mobile amorphous regions, and the longer relaxation time (12.2 ms) is the characteristic relaxation time for the highly ordered crystalline phase.

According to a proposal by Veeman et al.,[23] longer relaxation times reflect a spin−diffusion time which measures the time that magnetization requires to diffuse from a region with long relaxation times into a region with shorter relaxation times. Under this assumption, the average relative size of a crystalline domain may be estimated from the diffusion models used. If spin diffusion occurs in three dimensions, the average crystalline domain size may be calculated[24] from $\langle x \rangle = (6Dt)^{1/2}$, where D is the spin−diffusion coefficient and t is the longer relaxation component (12.2 ms). The spin−diffusion coefficient is estimated to be 5×10^{-12} cm^2/s for PET[24] and should be twice that value when used in a $T_{1\rho}(^1H)$ experiment.[23,24] Using the above model and parameters, the average crystalline domain size for PET2 is estimated to be 86 Å. However, the sizes of noncrystalline regions with shorter relaxation times (3.4−5.4 ms; cf. Table 6) are estimated to be around 50 Å.

Apparent crystallite sizes of 42 and 10 Å for PET2 and PET0, respectively, were estimated with the WAXD data using the Scherrer equation. The X-ray crystal lengths agree qualitatively with NMR crystallite sizes. The difference between X-ray and NMR results can be attributed to many assumptions made in the apparent crystal size boundaries for the two methods. However, the results from both methods show similar trends in apparent crystal sizes in PET upon SCF CO_2 treatments.

Summary and Conclusions

The molecular structure and mobility of PET before and after the treatment have been carefully characterized using NMR and X-ray spectroscopy. The results from both methods indicate the crystallinity of PET has increased from an essentially amorphous to a semicrystalline polymer during the SCF CO_2 treatment. This treatment, as mentioned above, is more efficient for PET than the previously reported CO_2 gas sorption treatment.

The glass transition temperature of PET is reduced due to the sorption of CO_2 at elevated pressure.[6,7,11] If the reduction of the glass transition temperature is large enough to put the system at the crystallization temperature, the polymer chains rearrange themselves into the conformations with lower free energies. Thus, the gauche conformation of aliphatic carbons in PET would be expected to convert to the trans conformation. This has been successfully detected using NMR data reported in this paper. Lambert and Paulaitis[13] attempted to separate the pressure effects on the CO_2-induced crystallization of PET from the gas sorption effects and concluded that the applied pressure controls crystallization kinetics at a pressure above 60 bar at 35 °C. It is believed that pressure effects also play an important role in the SCF CO_2 treatment under our experimental conditions.

Sawan et al.[2,3] measured the weight change of PET upon the SCF CO_2 treatment under similar experimental conditions to those described in this paper. A 2.02% weight gain in PET was noted immediately after the treatment. This percentage was reduced to 0.24% after 4 days and to 0.13% after 7 days from the time of treatment. The remaining 0.13% continued for 11 days, and it is safe to assume that some minimal amount of CO_2 was left in our PET samples when they were analyzed. The change in molecular mobility observed for PET is assumed to result from the morphological changes at the time of the SCF CO_2 treatment rather than from the residual trace amount of CO_2 in the polymer.

The molecular motional information for PET samples has been obtained from solid state ^{13}C relaxation experiments. Three different structural regimes (crystalline, rigid amorphous, and mobile amorphous) along with their motional characteristics have been identified from a combination of chemical shifts and partially relaxed spectra using spin−lattice relaxation (T_1) experiments for the SCF CO_2-treated PET sample. It was found that the rigid amorphous and crystalline domains have similar ^{13}C T_1 relaxation times, while mobile amorphous domain has a much shorter ^{13}C T_1 relaxation time. The experimental measurements and theoretical calculations of ^{13}C chemical shift principal values demonstrate that the structures of aliphatic carbons in the crystalline and the amorphous domain are dominated by the trans and gauche conformations, respectively. The previous assumption that amorphous PET

has two distinguishable motional regimes (rigid amorphous and mobile amorphous) was confirmed by the ^{13}C relaxation times in the rotating frame. A long $T_{1\rho}(^{13}C)$ component was observed for the SCF CO_2 treated PET sample, representing the crystalline phases. Using the three-motional-regime model, the NMR crystallinities were determined to be 51% and 75% for the aliphatic and protonated aromatic carbons, respectively. This qualitatively agrees with the crystallinity results determined from the WAXD. From the proton relaxation data in the rotating frame, the average crystalline domain size is estimated to be 86 Å for the SCF CO_2-treated PET sample, which is somewhat higher than that estimated using X-ray data.

Acknowledgment. We acknowledge Dr. Samuel P. Sawan for providing the SCF CO_2-treated poly(ethylene terephthalate) samples. Helpful discussions with Dr. Mark S. Solum are acknowledged. This work was supported at the University of Utah by Basic Energy Sciences at DOE through grant DE FG02-94ER14452 and at Los Alamos National Laboratory by the EPA Environmental Technologies Initiative through grant EPA/IAG DW89936500-01.

References and Notes

(1) McHugh, M. A.; Krukonis, V. J. *Supercritical Fluid Extraction: Principle and Practice*, 2nd ed.; Butterworth-Heinemann, Boston, 1994.
(2) Shieh, Y.-T.; Su, J.-H.; Manivannan, G.; Lee, P. H. C.; Sawan S. P.; Spall. W. D. *J. Appl. Polym. Sci.* **1996**, *59*, 695.
(3) Shieh, Y.-T.; Su, J.-H.; Manivannan, G.; Lee, P. H. C.; Sawan, S. P.; Spall, W. D. *J. Appl. Polym. Sci.* **1996**, *59*, 707.
(4) Watkins, J. J.; McCarthy, T. J. *Macromolecules* **1995**, *28*, 4067.
(5) Berens, A. R.; Huvard, G. S.; Korsmeyer, R. W.; Kuning, F. W. *J. Appl. Polym. Sci.* **1992**, *46*, 231.
(6) Chiou, J. S.; Barlow, J. W.; Paul, D. R. *J. Appl. Polym. Sci.* **1985**, *30*, 3911.
(7) Chiou, J. S.; Barlow, J. W.; Paul, D. R. *J. Appl. Polym. Sci.* **1985**, *30*, 2633.
(8) Condo, P. D.; Johnston, K. P. *J. Polym. Sci., Part B: Polym. Phys.* **1994**, *32*, 523.
(9) Handa, Y. P.; Roovers, J.; Wang, F. *Macromolecules* **1994**, *27*, 5511.
(10) Condo, P. D.; Johnston, K. P. *Macromolecules* **1992**, *25*, 6730.
(11) Mizoguchi, K.; Hirose, T.; Naito, Y.; Kamiya, Y. *Polymer* **1987**, *28*, 1298.
(12) Kamiya, Y.; Hirose, T.; Naito, Y.; Mizoguchi, K. *J. Polym. Sci., Polym. Phys. Ed.* **1988**, *25*, 159.
(13) Lambert, S. M.; Paulaitis, M. E. *J. Supercrit. Fluids* **1991**, *4*, 15.
(14) O'shea, K. E.; Krimse. K. M.; Fox, M. A.; Jonhston, K. P. *J. Phys. Chem.* **1991**, *95*, 7863.
(15) Kazarian, S. G.; Vincent, M. F.; Bright, F. V.; Liotta, C. L.; Eckert, C. A. *J. Am. Chem. Soc.* **1996**, *118*, 1729.
(16) Hirose, T.; Mizoguchi, K.; Kamiya, Y.; Terada, K. *J. Appl. Polym. Sci.* **1989**, *37*, 1513.
(17) Rohr, K. S.; Spiess, H. W. *Multidimensional Solid-State NMR and Polymers*; Academic Press: London, 1994.
(18) McBrierty, V. J.; Packer, K. J. *Nuclear Magnetic Resonance in Solid Polymers*; Cambridge University Press: Cambridge, 1993.
(19) (a) Sefcik, M. D.; Schaefer, J.; Stejakal, E. O.; McKey, R. A. *Macromolecules* **1980**, *13*, 1132−1137. (b) Schaefer, J.; Stejskal, E. O.; Steger, T. R.; Sefick, M. D.; McKey, R. A. *Macromolecules* **1980**, *13*, 1121.
(20) English, A. D. *Macromolecules* **1984**, *17*, 2182.
(21) Chmelka, B. F.; Schmidt-Rohr, K.; Spiess, H. W. *Macromolecules* **1993**, *26*, 2282.
(22) Asakura, T.; Konakazawa, T.; Demura, M.; Ito, T.; Marushashi, Y. *Polymer* **1996**, *37*, 1965.
(23) Gabriëlse, W.; Gaur, H. A.; Feyen, F. C.; Veeman, W. S. *Macromolecules* **1994**, *27*, 5811.
(24) Havens, J. R.; VanderHart, D. L. *Macromolecules* **1985**, *18*, 1663.
(25) Gan, Z. *J. Am. Chem. Soc.* **1992**, *114*, 8307.
(26) Hu, J. Z.; Orendt, A. M.; Alderman, D. W.; Pugmire, R. J.; Grant, D. M. *Solid State NMR* **1994**, *3*, 181.
(27) Hu, J. Z.; Wang, W.; Liu, F.; Solum, M. S.; Pugmire, R. J.; Ye, C.; Grant, D. M. *J. Magn. Reson., Ser. A* **1995**, *113*, 210.
(28) (a) Cobbs, W. H.; Burton, R. I. *J. Polym. Sci.* **1953**, *10*, 275. (b) Hsiung, C.-M *Trends Polym. Sci. (Cambridge, U.K.)* **1996**, *4*, 342.
(29) Jade v.3.1, Material Data, Inc., 1997.
(30) Alderman, D. W.; Solum, M. S.; Grant, D. M. *J. Chem. Phys.* **1986**, *84*, 3717.
(31) Fu, Y.; Busing, W. R.; Affholter, K. A.; Wunderlich, B. *Macromolecules* **1993**, *26*, 2187.ment
(32) POWD12 Software, Smith, D. K., Department of Ceosciences, The Pennsylvania State University, 1987.
(33) Huisman, R.; Heuvel, H. M. *J. Appl. Polym. Sci.* **1989**, *37*, 595.
(34) Hu, J. Z.; Pugmire, R. J.; Grant, M. D. Unpublished results.
(35) Henrichs, P. M. *Macromolecules* **1987**, *20*, 2099.
(36) Murphy, P. D.; Taki, T.; Gerstein, B. C.; Henrichs, P. M.; Massa, D. J. *J. Magn. Reson.* **1982**, *49*, 99.
(37) Mehring, M. *Principles of High-Resolution NMR in Solids*, 2nd ed.; Springer-Verlag: Berlin, Heidelberg, New York, 1983.
(38) Frisch, M. J.; Trucks, G. W.; Schegel, H. B.; Gill, P. M. W.; Jonnson, B. G.; Robb, M. A.; Cheeseman, J. R.; Keith, T. A.; Petersson, G. A.; Montgomery, J. A.; Raghavachari, K.; Al-Laham, M. A.; Zakrzewski, V. G.; Ortiz, J. V.; Foresman, J. B.; Ciolowski, J.; Stefanov, B. B.; Nanayakkara, A.; Challacombe, M.; Peng, C. Y.; Ayala, P. Y.; Chen, W.; Wong, M. W.; Andres, J. L.; Replogle, E. S.; Gomperts, R.; Martin, R. L.; Fox, D. J.; Binkley, J. S.; Defrees, D. J.; Baker, J.; Stewart, J. P.; Head-Gordon, M.; Gonzales, C.; Pople, J. A. *Gaussian 94*, Revision A.1; Gaussian, Inc.: Pittsburgh, PA, 1995.
(39) Ditchfield, R. *Mol. Phys.* **1974**, *27*, 789.
(40) Dunning, T. H. *J. Chem. Phys.* **1970**, *53*, 2823.
(41) Daubeny, R. de; Bunn, C. W.; Brown, C. J. *Proc. R. Soc. London* **1954**, *226A*, 531.
(42) Henrichs, P. M.; Tribone, J.; Massa, D. J.; Hewitt, J. M. *Macromolecules* **1988**, *21*, 1282.

MA9715031